Polarization-Insensitive Four-Wave-Mixing-Based Wavelength Conversion in Few-Mode Optical Fibers

Omar F. Anjum ⓘ, Massimiliano Guasoni, Peter Horak ⓘ, Yongmin Jung ⓘ, Periklis Petropoulos ⓘ, David J. Richardson ⓘ, *Fellow, IEEE, Fellow, OSA*, and Francesca Parmigiani ⓘ

Abstract—We report theoretical and experimental results on a wavelength converter based on intermodal phase matching in a graded index three-mode elliptical-core fiber. Here, two copolarized pump waves propagate in one spatial mode, whereas a signal and the corresponding generated idler propagate in another mode. We demonstrate that the idler power is independent of the signal polarization in both a 1 km and a 50 m long fiber. We attribute this polarization insensitivity to the fast random birefringence of the fiber under investigation in combination with the copolarized pump configuration.

Index Terms—Fiber nonlinear optics, four-wave mixing, higher order mode, optical signal processing, optical wavelength conversion.

Fig. 1. Schematic of the wave configuration and wavelength allocation of the IM FWM processes.

I. INTRODUCTION

FOUR-WAVE MIXING (FWM) is a well-known optical effect originating from electronic $\chi^{(3)}$ nonlinear processes that has been studied extensively as a mechanism for realizing ultra-fast all-optical signal processing. The earliest observation of FWM was made in a multimode fiber four decades ago [1], however optical signal processing applications today rely almost exclusively on single mode highly nonlinear fibers. This is primarily due to the maturity of engineered single mode fibers with very low values of dispersion and dispersion slope, making them excellent candidates for producing high FWM gain over broad bandwidths [2].

In recent years, interest in nonlinear effects in multimode fibers, specifically few mode fibers (FMFs), has resurfaced, primarily driven by developments in space division multiplexed communications [3]. Advances in fiber fabrication and the ability to independently launch and control high-order modes (HOMs) in FMFs have led to new studies of inter-modal (IM) FWM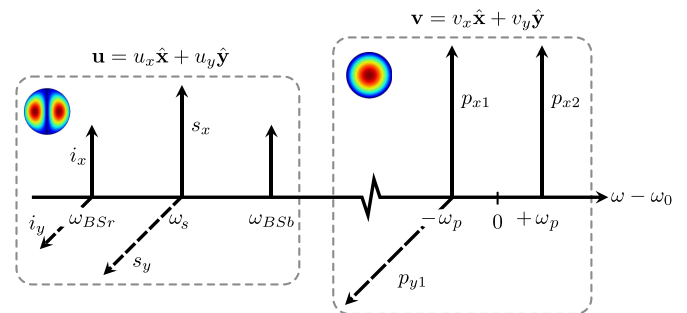 processes, in particular Bragg Scattering (BS) and Phase Conjugation (PC) [4]–[6]. By properly engineering the inverse group velocity (IGV) profiles of the supported modes of the FMF, it is possible to achieve broadband phase matching for either the BS [5], [6] or the PC [7] processes. Moreover, the selection of specific HOMs allows operation over multiple spectral bands, as demonstrated in [6]. This highlights an important potential advantage that FMFs can possess over their single mode counterparts. In [6], each pump was launched in a different spatial mode of a 1-km long elliptical core (EC) FMF (supporting three non-degenerate spatial modes: LP_{01}, LP_{11a} and LP_{11b}). Note that a circular fiber supporting three spatial mode groups could have also been used. This allowed the experimental demonstration of simultaneous wavelength and mode conversion of an input signal both within the C-band and from the C- to the L-band depending on the chosen mode for the second pump.

In this paper, using the same randomly birefringent EC-FMF, we change the configuration of the waves: the two pumps now excite the same spatial mode (LP_{01}) while the signal and the generated idlers propagate in a different mode (either LP_{11a} or LP_{11b}). The overall configuration of interacting waves is detailed in Fig. 1 and discussed further in the following section.

We then theoretically and experimentally study the sensitivity of IM FWM to signal polarization when the two pumps are co-polarized in such a configuration and examine the effect of the fiber length by experimenting with 1 km and 50 m samples of the same fiber. Finally, the influence of the relative polarization state between the pumps (i.e., co- and cross-polarized pumps) on the signal wavelength conversion is characterized.

The authors are with the Optoelectronics Research Centre, University of Southampton, Southampton SO17 1BJ, U.K. (e-mail: o.f.anjum@soton.ac.uk; m.guasoni@soton.ac.uk; peh@orc.soton.ac.uk; ymj@orc.soton.ac.uk; pp@orc.soton.ac.uk; djr@orc.soton.ac.uk; frp@orc.soton.ac.uk).

II. THEORETICAL FRAMEWORK

In order to get a physical insight into the wavelength conversion process, we develop a basic theoretical description of the corresponding IM FWM processes. Here we consider fibers that exhibit random birefringence fluctuations along their lengths. The light propagation dynamics in such fibers is strongly dependent on the ratio between the length scale of the random fluctuations L_C, and the set of beat-lengths L_B related to the pairs of quasi-degenerate modes [8]. In the fiber under test (FUT), we have three distinct and independent spatial modes, namely LP_{01}, LP_{11a} and LP_{11b}, each with double-degeneracy due to the two orthogonal polarizations. Whenever $L_C \gg \max L_B$, the random spatial fluctuations in the fiber are slow enough not to induce any appreciable random coupling between the polarizations within each mode. In this regime light propagates as in a fiber with fixed axes of birefringence (hereupon referred to as a 'birefringent fiber'). The same applies whenever the fiber length L is shorter than L_C. On the contrary, when L_C is of the same order as or shorter than $\min\{L_B\}$, and in addition $L_C \ll L$, then the randomness plays an important role (we refer to this as a 'randomly birefringent fiber'). In this regime the system dynamics is well described by the Manakov model [8].

In both types of fibers, birefringent and randomly birefringent, the light propagation is described by a set of coupled Nonlinear Schrödinger Equations (NLSEs) [9], [10]. As illustrated in Fig. 1, we indicate with v_j, u_j and q_j the slowly varying envelope of the j-polarized mode ($j \in x, y$) for the modes LP_{01}, LP_{11a} and LP_{11b}, respectively. Assuming the input signal and the generated idler waves propagating in the LP_{11} mode group to be much weaker than the pump waves in LP_{01} we can ignore the nonlinear terms induced by them [11], i.e., we ignore all the nonlinear terms that include $|u_j|^2$ and $|q_j|^2$. The set of NLSEs for the LP_{01} and LP_{11a} modes then take the following simplified form:

$$i\frac{\partial v_x}{\partial z} + i\beta_{1vx}\frac{\partial v_x}{\partial t} + \beta_{2vx}\frac{\partial^2 v_x}{\partial t^2} - \gamma\left(a|v_x|^2 + b|v_y|^2\right)v_x = 0 \tag{1}$$

$$i\frac{\partial u_x}{\partial z} + i\beta_{1ux}\frac{\partial u_x}{\partial t} + \beta_{2ux}\frac{\partial^2 u_x}{\partial t^2} - \gamma_{uv}\left(c|v_x|^2 + d|v_y|^2\right)u_x = 0 \tag{2}$$

where $\{\beta_{1uj}, \beta_{1vj}\}$ and $\{\beta_{2uj}, \beta_{2vj}\}$ are the IGVs and the group velocities (GVDs), respectively, of the j-polarization of the corresponding mode groups (LP_{01} and LP_{11a}). γ is the Kerr-nonlinear coefficient related to mode LP_{01} and, γ_{uv} is the coefficient related to the inter-modal nonlinear interaction between v and u [12]. The corresponding IGVs and GVDs, obtained from the a Taylor expansion around the average frequency of the two pump frequencies that we set as our reference frequency ($\omega = 0$), are evaluated at the two pumps and signal frequencies ($\pm\omega_p$ and ω_s, see Fig. 1). In a birefringent fiber $a = c = 1$ and $b = d = 2/3$ whereas in a randomly birefringent fiber $a = b = 8/9$ and $c = d = 4/3$ [9]. Two similar sets of equations can be re-written for the y-polarization mode and

for the LP_{01} and LP_{11b} mode pair after exchanging the labels $x \leftrightarrow y$ in (1) and for the amplitudes $u_j \leftrightarrow q_j$ respectively.

It should be noted that in a randomly birefringent fiber the local principal axes x and y change randomly and continuously along the fiber length [10]. Moreover, according to the Manakov model, when the polarization-mode dispersion is negligible (which is typically the case in few-km long fibers), the modal wavevectors are constant and independent of the polarization, that is, $\beta_{ux} = \beta_{uy}$, $\beta_{vx} = \beta_{vy}$ [13]. The electric field $v_j(z, t)$, consisting of the pump waves can be written as

$$v_j(z, t) = p_{j1}(z)\exp(-i\omega_p t) + p_{j2}(z)\exp(i\omega_p t) \tag{3}$$

where p_{j1} and p_{j2} are the field amplitudes of the pumps centered at $-\omega_p$ and $+\omega_p$, respectively.

The field $u_j(z, t)$ can be written as a linear combination of the signal $s_j(z)$ at ω_s, and the phase-matched idler, $i_j(z)$ at the red-shifted frequency ω_{BSr}:

$$\omega_{BSr} = \omega_s - 2\omega_p \tag{4}$$

$$u_j(z, t) = s_j(z)\exp(i\omega_s t) + i_j(z)\exp(i\omega_{BSr}t) \tag{5}$$

Note that the other generated idler centered at the blue-shifted frequency $\omega_{BSb} = \omega_s + 2\omega_p$, could be derived by solving similar equations. However, because this process is phase matched only for a very narrow band of frequencies [6], it is not discussed further here. Inserting $v_j(z, t)$ and $u_j(z, t)$ in (1), we find a system of linear differential equations describing a BS process where the energy is mutually exchanged between the signal and idler harmonics [13]. The initial condition for the signal is $s_j(z = 0) = s_{j0}$ with s_{j0} being the amplitudes of the injected signal along the x- and y-axes. The idler is absent at the fiber input, therefore $i_j(z = 0) = 0$.

We assume that the input pump components have the same power ($|p_{j1}(0)|^2 = |p_{j2}(0)|^2 = P$) and are linearly copolarized along the x-axis. After some algebraic manipulation we find that the magnitudes of $i_x(z)$ and $i_y(z)$ read as:

$$|i_x(z)| = c|s_{x0}|\gamma_{uv}Pz\,\text{sinc}(k_x z) \tag{6}$$

$$|i_y(z)| = d|s_{y0}|\gamma_{uv}Pz\,\text{sinc}(k_y z) \tag{7}$$

where

$$k_x^2 = \Delta\beta_x^2 + (c\gamma_{uv}P)^2 \tag{8}$$

$$k_y^2 = \Delta\beta_y^2 + (d\gamma_{uv}P)^2 \tag{9}$$

$$\Delta\beta_j = -\beta_{vx}(-\omega_p) + \beta_{vx}(\omega_p) + \beta_{uj}(\omega_{BSr}) - \beta_{uj}(\omega_s) \tag{10}$$

$\Delta\beta_j$ is the phase mismatch term related to the BSr process, whereas $\beta_{uj}(\omega)$ and $\beta_{vj}(\omega)$ are the wavevectors of the LP_{01} and LP_{11a} mode group computed at the frequency ω. Note that for the pump we only employ wavevectors $\beta_{vx}(\pm\omega_p)$, as both pumps are assumed to be x-polarized.

As previously mentioned, in randomly birefringent fibers, the wavevectors are identical in the x and y polarizations, thus $k_x = k_y$. From (6) we see that the total power P_I of the generated idler, that is $P_I = |i_x(z)|^2 + |i_y(z)|^2$, depends on the input signal polarization in a birefringent fiber. On the contrary,
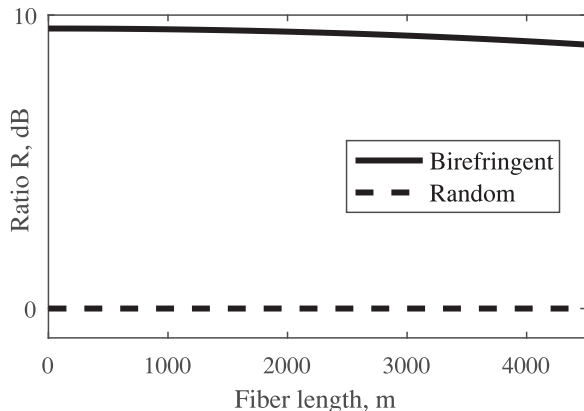
Fig. 2. Ratio R as a function of the fiber length in a birefringent or randomly birefringent fiber where $\gamma_{uv} = 0.71/(km\ W)$ and for an input pump power of 20.5 dBm per pump.

in a randomly birefringent fiber, the total idler power only depends on the total input signal power $|s_{x0}|^2 + |s_{y0}|^2$, but not on its original state of polarization. Fig. 2 displays the ratios $R = P_{I\parallel}/P_{I\perp}$ in both types of fibers, where $P_{I\parallel}$ is the idler power when the input signal and the pumps are co-polarized, whereas $P_{I\perp}$ is the idler power when the input signal and the pump are cross-polarized. $P_{I\parallel}$ and $P_{I\perp}$ are obtained from (6) assuming $\gamma_{uv} = 0.71/(km\ W)$ and $P = 20.5$ dBm per pump, following the values used in the actual experiment reported later. We observe a variation of up to 9.5 dB between the co-and cross-polarized instances for the birefringent fiber case, confirming the strong dependence of the idler growth on the signal polarization.

More generally, $R > 9$ dB for a fiber length up to 4.5 km. On the contrary, in randomly birefringent fibers the idler growth is independent of the signal polarization, therefore R is unitary (0 dB) regardless of the fiber length (see Fig. 2).

Further analysis of the BSr process for the randomly birefringent fiber case that does not assume identical polarization directions for the two pumps (not detailed here) reveals that the idler growth strongly depends on the relative state of polarization of the pumps: it is maximized when the pumps are co-polarized and it vanishes when they are orthogonally polarized.

III. EXPERIMENTAL SETUP

The experimental set-up we used to explore these predicted polarization properties is shown in Fig. 3(a) for the input configuration of the pumps and signal illustrated in Fig 1. Three continuous-wave tunable lasers are used to generate the two pumps and the signal. To obtain a high peak power (after amplification) and to avoid stimulated Brillouin scattering in the FUT [14], all three sources are gated with a 10% duty cycle at a repetition rate of 10 MHz, following which they are adjusted for temporal overlapping at the fiber input. In the case where the pumps are co-polarized, both pumps (about 20.5 dBm each at the input to the FUT) are coupled together before being launched into the pulse-carver. The signal wave (typically 15 dB lower than each pump) is launched into the LP_{11a} or LP_{11b} mode using a mode-multiplexer (MMUX) based on a free-space

phase plates (PP) [5]. The EC FMF axes are suitably aligned with the PP to achieve efficient coupling and the signal state of polarization is controlled using polarization controllers (PCs). Two different fiber lengths are considered: 1 km and 50 m. The mode-demultiplexer (MDMUX) is based on the same technology and directs light from each mode into an optical switch to obtain output spectra; a modal purity better of than 20 dB can be achieved using the MMUX and MDMUX. Note that for demonstrating the difference between co- and cross-polarized pumps only, the pump pulse-carvers and the PBS were removed and a third PC was added in one of the pump arms. This represented the simplest modification of the set-up for this purpose.

Fig. 3(b) shows the relative IGV (RIGV) of the modes obtained by a time-of-flight measurement. As previously mentioned, the 10% ellipticity of the fiber core breaks the degeneracy of the LP_{11} spatial modes (the two spatial modes of the LP_{11} group are well separated), but it does not break the polarization degeneracy. In other words, in the graded-index FUT, modes of different groups are decoupled, whereas the polarization modes within the same group remain coupled, so that relevant energy exchange occurs among them [15]. The difference in wavelength when any mode pairs have the same RIGV, indicating the conditions for phase-matching [4], is about 25 nm (40.6 nm) for the LP_{01}-LP_{11a} (LP_{01}-LP_{11b}) pair. This was achieved by linearly fitting the measured IGV curves and extrapolating the data beyond the measured band.

The effective areas for modes of groups LP_{01} and LP_{11} are 87 μm^2 and 123 μm^2 respectively. Since the modes of graded-index fibers can be approximated as Hermite-Gaussian functions [16], we can estimate their transverse profiles from their effective areas. Finally, the inter-modal Kerr coefficient γ_{uv} is computed from the knowledge of the transverse profiles (see e.g., [12]).

IV. EXPERIMENTAL RESULTS

Typical spectra around the wavelengths of interest (pumps in the LP_{01} and signal in either the LP_{11a} or LP_{11b}) are shown in Fig. 4 when the 1 km EC FMF is used, where different spectra at the LP_{01}, LP_{11a} and LP_{11b} MDMUX ports are reported in the same figure for easier comparison. Pump 1 wavelength is (always fixed) at 1537.4 nm and Pump 2 wavelength in Fig. 4 is 1539.9 nm (hence a detuning of 2.5 nm). The signal is always launched in the LP_{11a} mode at 1562.4 nm and in the LP_{11b} mode at 1578 nm. The spectrum at the LP_{01} MDMUX port shows the presence of the pumps together with the generated intra-modal FWM idlers, while the spectra at the LP_{11a} and LP_{11b} MDMUX ports show the presence of the signals together with their corresponding generated inter-modal FWM idlers (labelled BSr and BSb in the figure) lying in the C-band and L-band, respectively. The phase-matched BSr idlers in both LP_{11} modes are about 20 dB stronger than the non-phase-matched BSb, implying that this wavelength conversion scheme can allow efficient and controlled conversion between specified wavelength channels. This could have a clear benefit in terms of avoiding contamination of the signal with undesired generated idlers that may eventually overlap with other signals (usually referred to as 'nonlinear
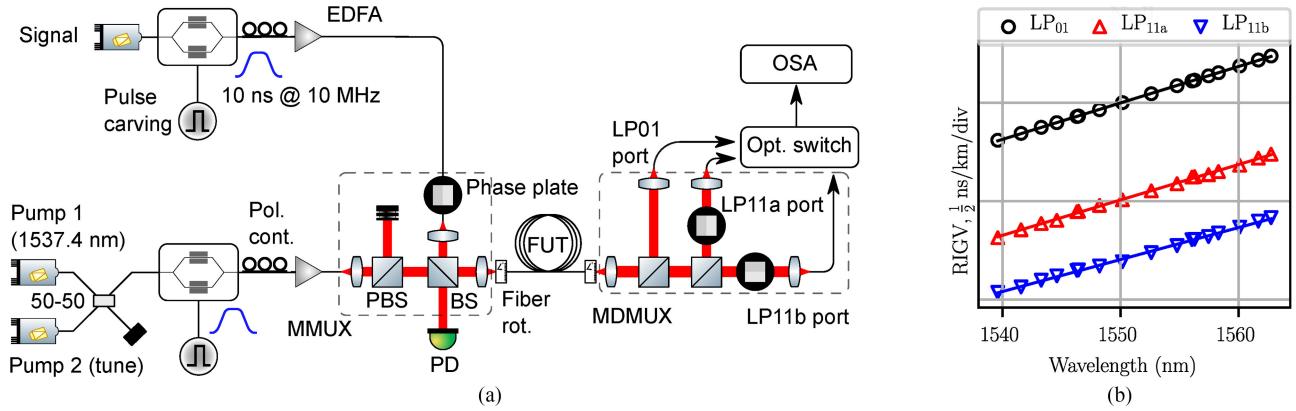
Fig. 3. (a) Experimental setup of intermodal FWM in the elliptical core few mode fiber supporting the LP_{01}, LP_{11a}, and LP_{11b} modes. (b) Measured RIGV curves of the fiber modes.
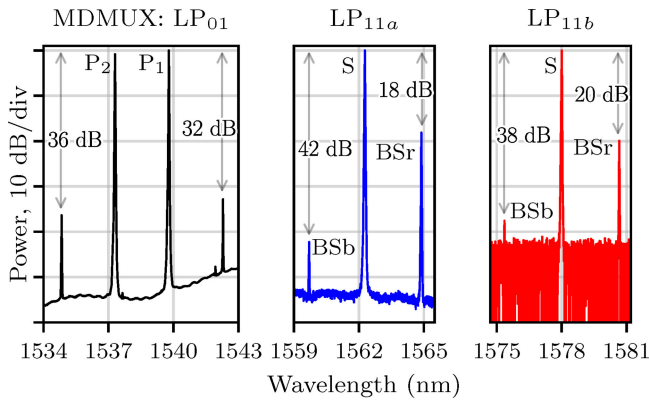

Fig. 4. Composite of normalized spectra after 1 km of FUT, collected at the LP_{01}, LP_{11a}, and LP_{11b} MDMUX output ports with signal wavelengths of 1562.4 nm and 1578 nm and pump-to-pump detuning of 2.5 nm.

Fig. 5. (a) and (b) show the CEs of the BSr process in the 1 km fiber for the LP_{11a} and LP_{11b} modes, respectively. (c) and (d) show CEs of the BSb process in the 1 km fiber for the LP_{11a} and LP_{11b} modes, respectively.

cross-talk'), if wavelength division multiplexed signals are to be investigated.

Using the 1 km sample of the FUT, the signal was then kept either co- or cross-polarized (referred to as 'co-pol' and 'cross-pol' in Fig. 5) relative to the two co-polarized pumps at the input of the FUT. With reference to Fig. 1, this would be an interaction between the input waves $\{s_x$ or $s_y, p_{1x}, p_{2x}\}$ and the idler will therefore be i_x or i_y. The conversion efficiency (CE) as a function of pump-to-pump wavelength detuning was measured for both the LP_{11a} and LP_{11b} modes. The CE was calculated as the difference in dB between the generated idlers at the output of the FUT and the input signal. As expected [6], in both cases the phase-matched BSr process shows a broader bandwidth (almost 2 nm at -6 dB for the LP_{11a}) than the BSb process (about 1 nm at -6 dB for the LP_{11a}) with a maximum CE of about -2.5 dB for both cases.

More importantly, the CEs for both processes are found experimentally to be largely independent of the signal polarization: the largest difference in CE between the co- and cross-polarized cases is 2 dB, further reduced to 0.7 dB when lower pump powers (15 dBm per pump) were used (not shown here). We conjecture that this small CE difference and its power dependence are due to drifts of the polarization between the pumps and the modal
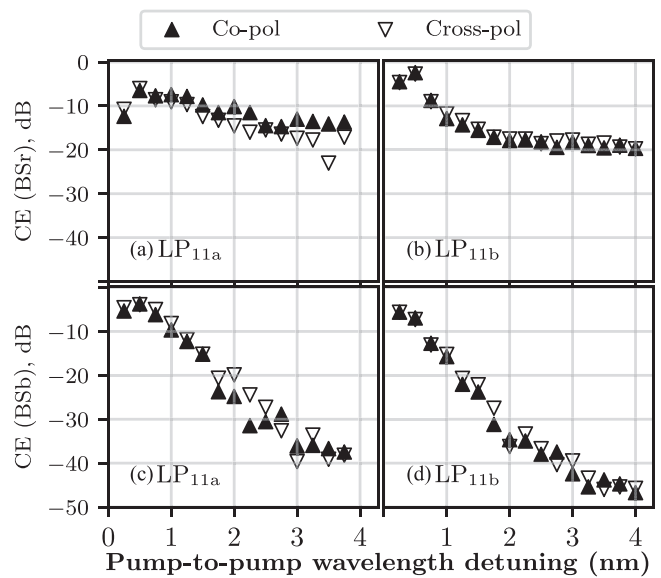
purity during the experiment, which are more severe at higher pump powers.

Away from the phase matching, the CE variation between the co/cross cases increases. In all instances, these measured values are compatible with our theoretical estimate for randomly birefringent fibers ($R = 0$ dB) rather than for birefringent fibers ($R = 9.5$ dB). Note that the experimental results were obtained in a stable and repeatable manner over time, in contrast to the observations in [17], where power fluctuations of the idlers generated by these processes were noted.

Similar CE measurements were carried out using a shorter length (50 m) of the same fiber and the same launched pump powers (20.5 dBm per pump). The corresponding results for the LP_{11a} and LP_{11b} modes are reported in Fig. 6. The maximum CE drops to about -28 dB in this case because of the shorter interaction length, but the -6 dB bandwidth of the BSr increases to about 3 nm. The maximum CE variation with the state of polarization of the signal is about 1 dB.
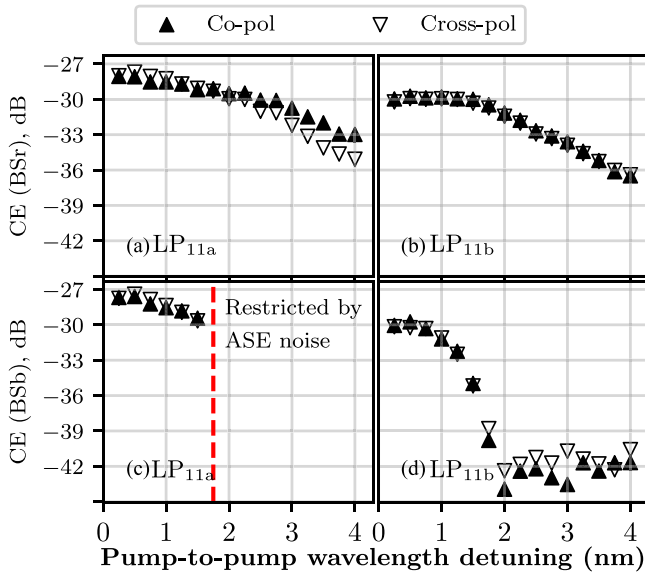
Fig. 6.   (a) and (b) show CEs of the BSr process for the 50 m fiber modes LP_{11a} and LP_{11b}. (c) and (d) show CEs for the BSb processes for these modes.
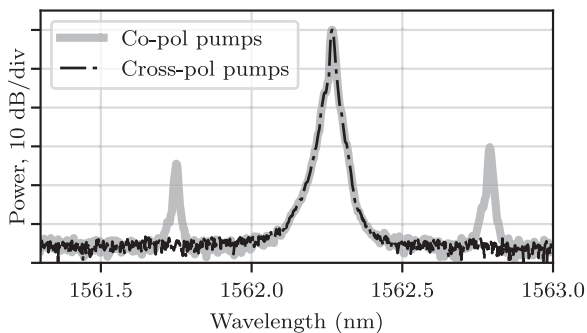

Fig. 7.   IM FWM spectra at the LP_{11a} MDMUX output port for copolarized and cross-polarized pumps.

As in the 1 km long fiber, this indicates near polarization-independence of the conversion dynamics, and thus a randomly birefringent nature of the 50 m long fiber. We therefore conjecture that the length scale L_C of random fluctuations is much shorter than 50 m. It is worth noting that, should the fiber length be $L \ll L_C$, we would have a (fixed axes) birefringent fiber where strong polarization dependence (up to 9.5 dB) would be observed. However, such short fiber lengths would give FWM idlers much below the experimental noise floor.

Finally, we studied the influence of the relative state of polarization of the pumps on the IM-FWM process using the 1-km long fiber. In particular, the pumps were set to be co- or orthogonally polarized to one another by modifying the set-up as previously discussed. With reference to Fig. 1, now the inputs to the FUT are the waves $\{s_x + s_y, p_{x1} \text{ or } p_{y1}, p_{x2}\}$. The corresponding spectra are reported in Fig. 7, when the signal excites the LP_{11a} mode and the pump-to-pump wavelength detuning was set to 0.5 nm. As the theory predicts, if the pumps are orthogonally polarized, no observable IM-FWM idlers are generated, regardless of the state of the signal polarization. This is not the case for co-polarized pumps where a CE of about

-30 dB is observed with an optical signal to noise ratio better than 20 dB.

V. CONCLUSION

We have theoretically and experimentally demonstrated polarization insensitive wavelength conversion based on inter-modal four wave mixing in both a 1 km and a 50 m long three-mode fiber. By launching two co-polarized pumps in the LP_{01} mode and the signal in either the LP_{11a} or LP_{11b} modes at the phase-matched wavelengths, conversion of signals in the C- or the L-band is achieved with a signal polarization sensitivity for the BS processes of less than 2 dB. If the two pumps are then chosen to be orthogonally polarized no IM-FWM idlers are generated. This polarization independence is consistent with the assumption of a randomly birefringent fiber, i.e., a fiber where the length scale of longitudinal fluctuations is shorter than the birefringence beat lengths of the relevant modes.

Bandwidths of up to 3 nm at -6 dB have been demonstrated and much broader bandwidths are expected in dispersion engineered fibers. Increasing the number of supported modes, signal bands that are further away can also be targeted.

REFERENCES

[1] R. H. Stolen, J. E. Bjorkholm, and A. Ashkin, "Phase-matched three-wave mixing in silica fiber optical waveguides," *Appl. Phys. Lett.*, vol. 24, no. 7, pp. 308–310, 1974. [Online]. Available: http://dx.doi.org/10.1063/1.1655195

[2] S. Radic *et al.*, "Continuous-wave parametric gain synthesis using nondegenerate pump four-wave mixing," *IEEE Photon. Technol. Lett.*, vol. 14, no. 10, pp. 1406–1408, Oct. 2002.

[3] D. J. Richardson, J. M. Fini, and L. E. Nelson, "Space-division multiplexing in optical fibres," *Nature Photon.*, vol. 7, no. 5, pp. 354–362, May 2013, review. [Online]. Available: http://dx.doi.org/10.1038/nphoton.2013.94

[4] R. J. Essiambre *et al.*, "Experimental investigation of inter-modal four-wave mixing in few-mode fibers," *IEEE Photon. Technol. Lett.*, vol. 25, no. 6, pp. 539–542, Mar. 2013.

[5] S. M. M. Friis *et al.*, "Inter-modal four-wave mixing study in a two-mode fiber," *Opt. Express*, vol. 24, no. 26, pp. 30 338–30 349, Dec. 2016. [Online]. Available: http://www.opticsexpress.org/abstract.cfm?URI=oe-24-26-30338

[6] F. Parmigiani *et al.*, "C- to l- band wavelength conversion enabled by parametric processes in a few mode fiber," in *Proc. Opt. Fiber Commun. Conf*, Opt. Soc. Amer., 2017, p. Th1F.4. [Online]. Available: http://www.osapublishing.org/abstract.cfm?URI=OFC-2017-Th1F.4

[7] P. H. M. Guasoni, F. Parmigiani, and D. J. Richardson, "Novel fiber design for wideband conversion and amplification in multimode fibers," in *Proc. Eur. Conf. Opt. Comm.*, 2017, Paper P1.SC1.12.

[8] M. Guasoni, F. Parmigiani, P. Horak, J. Fatome, and D. J. Richardson, "Intermodal four-wave-mixing and parametric amplification in km-long multi-mode fibers," *J. Lightw. Technol.*, vol. 35, no. 24, pp. 5296–5305, Dec. 2017.

[9] M. Guasoni, "Generalized modulational instability in multimode fibers: Wideband multimode parametric amplification," *Phys. Rev. A*, vol. 92, Sep. 2015, Art no. 033849. [Online]. Available: https://link.aps.org/doi/10.1103/PhysRevA.92.033849

[10] S. Mumtaz, R.-J. Essiambre, and G. P. Agrawal, "Nonlinear propagation in multimode and multicore fibers: Generalization of the manakov equations," *J. Lightw. Technol.*, vol. 31, no. 3, pp. 398–406, Feb. 2013. [Online]. Available: http://jlt.osa.org/abstract.cfm?URI=jlt-31-3-398

[11] J. Nuño, M. Gilles, M. Guasoni, B. Kibler, C. Finot, and J. Fatome, "40 GHz pulse source based on cross-phase modulation-induced focusing in normally dispersive optical fibers," *Opt. Lett.*, vol. 41, no. 6, pp. 1110–1113, Mar. 2016. [Online]. Available: http://ol.osa.org/abstract.cfm?URI=ol-41-6-1110

[12] F. Poletti and P. Horak, "Description of ultrashort pulse propagation in multimode optical fibers," *J. Opt. Soc. Amer. B*, vol. 25, no. 10, pp. 1645–1654, Oct. 2008. [Online]. Available: http://josab.osa.org/abstract.cfm?URI=josab-25-10-1645

[13] C. J. McKinstrie, S. Radic, and A. R. Chraplyvy, "Parametric amplifiers driven by two pump waves," *IEEE J. Select. Topics Quantum Electron.*, vol. 8, no. 3, pp. 538–547, May 2002.

[14] J. H. Lee *et al.*, "Experimental comparison of a kerr nonlinearity figure of merit including the stimulated Brillouin scattering threshold for state-of-the-art nonlinear optical fibers," *Opt. Lett.*, vol. 30, no. 13, pp. 1698–1700, Jul. 2005. [Online]. Available: http://ol.osa.org/abstract.cfm?URI=ol-30-13-1698

[15] F. Parmigiani, Y. Jung, L. Grner-Nielsen, T. Geisler, P. Petropoulos, and D. J. Richardson, "Elliptical core few mode fibers for multiple-input multiple output-free space division multiplexing transmission," *IEEE Photon. Technol. Lett.*, vol. 29, no. 21, pp. 1764–1767, Nov. 2017.

[16] L. Su, K. S. Chiang, and C. Lu, "Microbend-induced mode coupling in a graded-index multimode fiber," *Appl. Opt.*, vol. 44, no. 34, pp. 7394–7402, Dec. 2005. [Online]. Available: http://ao.osa.org/abstract.cfm?URI=ao-44-34-7394

[17] M. Esmaeelpour *et al.*, "Power fluctuations of intermodal four-wave mixing in few-mode fibers," *J. Lightw. Technol.*, vol. 35, no. 12, pp. 2429–2435, Jun. 2017. [Online]. Available: http://jlt.osa.org/abstract.cfm?URI=jlt-35-12-2429

Authors biographies not available at the time of publication.